

Human limb-specific and non-limb-specific brain representations during kinesthetic illusory movements of the upper and lower extremities

Eiichi Naito,^{1,2,3,*} Tokuro Nakashima,^{3,*} Tomonori Kito,³ Yu Aramaki,^{1,4,5} Tomohisa Okada⁴ and Norihiro Sadato^{4,5}

¹National Institute of Information and Communication Technology, Research Department 1, Kobe Advanced ICT Research Center, Biophysical ICT Group, Kyoto, 619-0288, Japan

²ATR Computational Neuroscience Laboratories, 2-2-2 Hikaridai, Seika-cho, Soraku-gun, Kyoto, 619-0288, Japan

³Graduate School of Human and Environmental Studies, Kyoto University, Sakyo-ku, Kyoto, Japan

⁴Department of Cerebral Research, Psychophysiology Section, National Institute for Physiological Sciences, Okazaki, Aichi, Japan

⁵JST (Japan Science and Technology Corporation)/RISTEX (Research Institute of Science and Technology for Society), Kawaguchi, Japan

Keywords: functional magnetic resonance imaging, kinesthetic illusion, motor somatotopy, normal volunteers, tendon vibration

Abstract

Sensing movements of the upper and lower extremities is important in controlling whole-body movements. We have shown that kinesthetic illusory hand movements activate motor areas and right-sided fronto-parietal cortices. We investigated whether illusions for the upper and lower extremities, i.e. right or left hand or foot, activate the somatotopical sections of motor areas, and if an illusion for each limb engages the right-sided cortices. We scanned the brain activity of 19 blindfolded right-handed participants using functional magnetic resonance imaging (fMRI) while they experienced an illusion for each limb elicited by vibrating its tendon at 110 Hz (ILLUSION). As a control, we applied identical stimuli to the skin over a nearby bone, which does not elicit illusions (VIBRATION). The illusory movement (ILLUSION vs. VIBRATION) of each immobile limb activated limb-specific sections of the contralateral motor cortex (along with somatosensory area 3a), dorsal premotor cortex (PMD), supplementary motor area (SMA), cingulate motor area (CMA), and the ipsilateral cerebellum, which normally participate in execution of movements of the corresponding limb. We found complex non-limb-specific representations in rostral parts of the bilateral SMA and CMA, and illusions for all limbs consistently engaged concentrated regions in right-sided fronto-parietal cortices and basal ganglia. This study demonstrated complete sets of brain representations related to kinesthetic processing of single-joint movements of the four human extremities. The kinesthetic function of motor areas suggests their importance in somatic perception of limb movement, and the non-limb-specific representations indicate high-order kinesthetic processing related to human somatic perception of one's own body.

Introduction

Sensing movements of the upper and lower extremities, i.e. right or left hand or foot, plays an important role when humans and animals control their extremities (Rothwell *et al.*, 1982; Bard *et al.*, 1995; Ghez & Sainburg, 1995; Sainburg *et al.*, 1995). The sensory afferents from muscle spindle, cutaneous, and joint receptors contribute to the signalling of limb movements to the brain (Burke *et al.*, 1988; Edin & Vallbo, 1988, 1990; Edin & Abbs, 1991; Edin & Johansson, 1995; Edin, 2004; Collins *et al.*, 2005), and the brain processes these sensory inputs to create perceptual representations of limb movements (Head & Holmes, 1911). The muscle spindle receptors are particularly sensitive to detect direction and speed of limb movements (Burke *et al.*, 1976, 1988; Edin & Vallbo, 1988, 1990; Ribot-Ciscar & Roll, 1998). Vibrating the tendon of a limb's muscle excites its muscle

spindle afferents (Goodwin *et al.*, 1972a, b; Burke *et al.*, 1976; Roll & Vedel, 1982; Gandevia, 1985; Roll *et al.*, 1989), and the brain receives and processes their inputs (Wiesendanger & Miles, 1982) so that people experience a sensation of slow movement as if the vibrated limb were moving (kinesthetic illusory limb movement) in the absence of actual movement, intention to move, or sense of effort (Burgess *et al.*, 1982; Matthews, 1982). In our series of human neuroimaging studies (Naito *et al.*, 1999, 2002a, b, 2005; Naito & Ehrsson, 2006), we have focused on investigating the brain mechanism underlying the illusion of hand movement, yet little is known about the mechanism related to the illusion of foot movement.

With regard to the illusory hand movement, we have consistently demonstrated that the illusion activates the hand sections of multiple motor areas, i.e. contralateral primary motor cortex (M1), dorsal premotor cortex (PMD), caudal parts of the supplementary motor (SMA) and cingulate motor areas (CMA) and ipsilateral cerebellum (Naito *et al.*, 1999, 2002a, b, 2005). Thus, one may predict that kinesthetic illusory foot movement also activates the limb-specific (foot) sections of these multiple motor areas in the absence of actual foot movements.

Correspondence: Dr Eiichi Naito, ¹National Institute of Information and Communication Technology, as above.

E-mail: enaito@atr.jp; eiichi.naito@nict.go.jp

*E.N. and T.K. contributed equally to this work.

Received 16 January 2007, revised 4 April 2007, accepted 11 April 2007

We also found in our previous study (Naito *et al.*, 2005) that the bilateral rostral SMA/CMA and right-sided fronto-parietal regions are commonly activated during the illusions irrespective of whether the illusion is experienced on the right or the left hand. Our interpretation of this finding was that activations in these regions probably reflect non-limb-specific representations related to high-order kinesthetic processing. Thus, if this view is correct, we may expect that the illusions for the upper and lower extremities, i.e. right or left hand or foot, consistently activate the bilateral rostral SMA/CMA and right-sided fronto-parietal cortices. This is important because if this is the case, we may assign these regions hierarchically high-order integrative roles in the perception of the dynamic configuration of limbs in intrapersonal space, which may relate to somatic perception of one's own body.

To address these questions, we measured brain activity (blood oxygenation-level dependent, BOLD) using functional magnetic resonance imaging (fMRI) to detect brain activity in 19 blindfolded right-handed participants while they experienced an illusion for each limb elicited by vibrating its tendon at 110 Hz (ILLUSION). In a control condition for the skin vibration, which may recruit vibro-tactile receptors (Johansson & Vallbo, 1983), we applied identical stimuli to the skin surface over a nearby bone beside the tendon, which does not elicit any illusions (VIBRATION). To identify brain areas related to the illusions, we compared activity during ILLUSION with that during VIBRATION.

Materials and methods

Participants

Nineteen healthy right-handed (Oldfield, 1971) participants (18 males and one female) aged 19–36 with no history of neurological or other diseases participated in this study. All participants had given their informed consent, and the Ethical Committee of the National Institute of Physiological Science had approved the study. The fMRI experiment was carried out following the principles and guidelines of the Declaration of Helsinki (1975).

Behavioural experiment

Before the fMRI experiment, outside the scanner, we evaluated the illusory experience of hand or foot movement. The participants lay comfortably on a bed in the supine position with their eyes closed and were requested to be aware of sensation from the vibrated limb. Their arms and legs were supported, and their hands and feet were completely relaxed and did not touch anything throughout the experiment. Thus, the participants were absolutely passive in all conditions.

For their hands, we vibrated the tendon of the extensor carpi ulnaris (ECU) muscle of the right or left hand for 30 s, which elicited illusory wrist flexion movement. For their feet, we vibrated the tendon of the tibialis anterior (TA) muscle of the right or left foot for 30 s, which elicited illusory ankle plantar-flexion. We used a non-magnetic vibrator (110 Hz) (ILLUSOR, Umihira Ltd, Kyoto, Japan), driven by constant air pressure provided by an air-compressor (AIR KING GTAC 1525, GREAT TOOL, Taipei). To elicit vivid illusory foot movement, we adopted an amplitude (± 3.5 mm) of vibration stimuli for both hands and feet. Identical stimuli were used during fMRI scanning. Each condition (vibrating of the tendon of the right or left hand or foot) was repeated three times in a randomised order. After the onset of vibration stimuli, when the participants started feeling illusory movement, they were asked to say, 'start', and if the illusions disappeared within 30 s they were asked to say, 'stop'. After each trial, the participants replicated the illusory movements by actually moving

each limb until the maximum illusory angle was reached. We measured the angles from the relaxed position with the aid of two small bars laterally attached to the skin surface of the hand or foot. The angle of these bars was read using a transparent protractor that was placed adjacent to the limb (Naito *et al.*, 2002a). As controls, we vibrated the skin surface over a nearby bone (i.e. the processus styloideus ulnae of the hand or lateral malleolus of the foot) for 30 s. Afterward, we asked the participants if they felt any illusory movement to confirm whether these stimuli produced any (Naito & Ehrsson, 2006). The contact surface on the skin was approximately 1 cm² for all vibration conditions. One experimenter operated the vibrator by manually applying it to the skin with a light pressure.

We calculated mean illusory angle and mean onset of illusion separately from the three trials in each participant. As statistical analyses, we conducted two-factorial [right, left (2) \times hand, foot (2); repeated measurement] analysis of variance (ANOVA) for the mean angle and for the mean onset separately.

To monitor changes in muscular activity during vibration, we recorded EMGs from the skin surface over the vibrated ECU and the flexor carpi ulnaris (FCU), which is an agonistic muscle to the illusory direction of the hand, and also from the vibrated TA and the soleus (SO; agonistic) muscle of the foot. A pair of 8-mm diameter Ag/AgCl electrodes (NT-211 U, Nihon Kohden, Tokyo, Japan) was placed on the skin surface over each muscle. The signals were amplified 2000 times using an amplifier (AB-610J, Nihon Kohden, Tokyo, Japan) and displayed on a PC monitor using special software (PowerLab/16SP, ADInstruments, Australia; see details in Kito *et al.* 2006). In almost half (approximately 40%) of all trials, irrespective of the vibrated limb, we observed no conspicuous muscular activity throughout the trial. Even in the remaining trials, we found that the increase was temporal within the trial and did not last throughout the tendon vibration. Thus, we only report changes of EMG activity in a purely descriptive manner in the results.

fMRI experiment

A 3.0 T SIEMENS scanner (MAGNETOM Allegra) with a head-coil provided T1-weighted anatomical images (3D-SPGR) and functional T2*-weighted echoplanar images (64 by 64 matrix, 3.0 mm by 3.0 mm, TE 40 ms). A functional image volume comprised of 44 3-mm thick slices was imaged, which ensured that the whole brain was within the 192-mm \times 192-mm field of view.

The blindfolded participants rested comfortably in the supine position in the MR scanner. Their extended arms were orientated in a relaxed position parallel to their torsos, and their limbs were completely relaxed. During the experiment, the participants were instructed to be aware of sensation from the vibrated limb, to relax their whole body, and to make no limb movements. In the fMRI experiment, they were not asked to replicate the illusory movements after each trial. They were also instructed to make no effort to remember illusory angles during scanning. Instead, after each session finished, the experimenter asked them whether they felt illusions or not for each vibration epoch (see below). After the whole experiment was completed, the experimenter asked them to retrospectively rate the strength of illusion for hand and foot (Naito *et al.*, 1999) in order to confirm that the hand-illusion is larger than the foot-illusion as we observed in the behavioural experiment. Thus, during scanning they were physically and mentally passive.

During fMRI scanning, three conditions were imposed. As in the behavioural experiment, we vibrated the skin surface over the tendon of the right hand, left hand, right foot, or left foot (ILLUSION) and

vibrated the skin surface over bone near each tendon (VIBRATION). In the third condition, no vibration stimuli were provided (REST). To provide instructions about the conditions and the onset and termination of the vibration to the experimenter, computer-generated visual cues were projected onto the white surface of the scanner (the blindfolded participants could not see this visual information).

For each participant, we conducted eight fMRI sessions, with two sessions assigned to each limb. The sessions were conducted in a pseudo-randomised order across participants. A total of 8×72 functional image volumes were collected for each participant. In each session for a limb, there were three conditions (ILLUSION, VIBRATION and REST). Each condition (epoch) lasted for 32 s (eight functional images, TR 4 s), and was repeated three times in each session. The order of conditions was also pseudo-randomised. To change the vibration site (tendon or bone) during a session, we included special periods that lasted 8 s, during which time the scanner continued to collect images. In the analysis, the data from these periods were modelled as conditions of no interest and therefore, not used.

Data analysis

The fMRI data was analysed with Statistical Parametric Mapping software (SPM99; <http://www.fil.ion.ucl.ac.uk/spm>; the Wellcome Department of Cognitive Neurology, London). The functional images were realigned to correct for head movements, coregistered with each participant's anatomical MRI and transformed (by linear and non-linear transformation) to the format of the Montréal Neurological Institute (MNI) standard brain (Naito & Ehrsson, 2006). The functional images were scaled to 100 and spatially smoothed with an 8-mm full width at half maximum (FWHM) isotropic Gaussian kernel, and smoothed in time by a 4-s FWHM Gaussian kernel. As we knew from the behavioural experiment before the fMRI experiment that the illusions started after a few seconds (see Results), we omitted the first 4 s of all conditions by defining these periods as conditions of no interest in the model. For each individual participant, we fitted a linear regression model (general linear model) to the data. Each condition was modelled with a boxcar function delayed by 4 s and convoluted with the standard SPM99 haemodynamic response function.

In the following analyses of fMRI data, we first defined a linear contrast (see below in each analysis) in a general linear model for each participant. The result of this analysis was the estimated BOLD signals for the contrast from each of the 19 participants (contrast images). To accommodate interparticipant variability, the contrast images from all participants were entered into a random effect group analysis (second level analysis; Friston *et al.*, 1999). One-sample *t*-test was used (18 degrees of freedom). A voxel-wise threshold of $T > 3.61$ ($P < 0.001$ uncorrected) was used to generate a cluster image.

Brain areas active during illusion of each limb

In the first-level individual analyses, we analysed a contrast between ILLUSION and VIBRATION (ILLUSION vs. VIBRATION) for a limb (Naito *et al.*, 2005). In the second level analysis, for statistical inference, we used a threshold of $P < 0.05$ or better at the cluster level after correction for multiple comparisons in the entire brain space. These analyses were performed for each limb. The results are summarized in Figs 1 and 2.

In the following regions-of-interest (ROI) analyses (see further below), we defined ROI based on the cluster images ($P < 0.05$ corrected) generated from this second level analysis.

Brain areas active during skin vibration of each limb

In the first-level individual analyses, we analysed a contrast (VIBRATION vs. REST) for each limb (Naito *et al.*, 2005). In the second level analysis, the same statistical threshold was used (see above). The results are shown in Fig. 3.

ROI analysis for limb-specific activation

Within the regions (ROI) active during illusion for a limb (ILLUSION vs. VIBRATION, $P < 0.05$ corrected; see Figs 1 and 2), regions exclusively active during illusion for a particular limb were further detected by contrasting illusion for a particular limb vs. illusions for other three limbs, e.g. $3 \times$ right hand (ILLUSION vs. VIBRATION) vs. [left hand (ILLUSION vs. VIBRATION) + right foot (ILLUSION vs. VIBRATION) + left foot (ILLUSION vs. VIBRATION)]. In the second level analysis, we searched for limb-specific activations in the ROI active during illusion for the particular limb, e.g. right hand (ILLUSION vs. VIBRATION). The same *T* threshold ($T > 3.61$) was used to generate a limb-specific cluster image, and we only report active clusters whose sizes are larger than 5 voxels (this threshold was used in the following ROI analyses). This approach ensures that activity in the ROI significantly increases during illusion for a particular limb, and thus activations specific to a particular limb can not merely be attributed to effect of deactivation during illusions for the other three limbs. These analyses were carried out for each limb, respectively. The results are tabulated in Table 2.

As shown in Figs 1 and 2, we found complex overlapping of activations during illusions. To statistically evaluate non-limb-specific activations, we performed further following ROI analyses.

ROI analysis for bimanual activation

Regions exclusively active during illusions for right and left hands were detected by contrasting illusions for both hands vs. illusions for both feet, i.e. [right hand (ILLUSION vs. VIBRATION) + left hand (ILLUSION vs. VIBRATION)] vs. [right foot (ILLUSION vs. VIBRATION) + left foot (ILLUSION vs. VIBRATION)]. In the second level analysis, we searched for bimanual activations in the ROI that was consistently active during right-hand illusion [right hand (ILLUSION vs. VIBRATION), $P < 0.05$ corrected; Figs 1 and 2] and during left-hand illusion [left hand (ILLUSION vs. VIBRATION)]. We generated the intersection (ROI) image between these two statistical images. The ROI included bilateral SMA/CMA and inferior frontal cortex, right inferior parietal cortex and basal ganglia. This approach ensures that activity in the ROI significantly and consistently increases during illusions for both right and left hands, and thus bimanual activations detected in this contrast exclusively reflects the illusions for both hands as compared to the illusions for both feet. The results are shown in Fig. 5.

We used the same approach using a reversed contrast to depict regions exclusively related to illusions for both feet. The ROI was the regions (bilateral SMA/M1, rostral CMA and inferior frontal cortices, right basal ganglia and thalamus) that were consistently active during right-foot illusion and during left-foot illusion (see above).

ROI analysis for limb-side activation

Regions exclusively active during illusions for right-sided limbs (hand and foot) were detected by contrasting illusions for right hand and foot

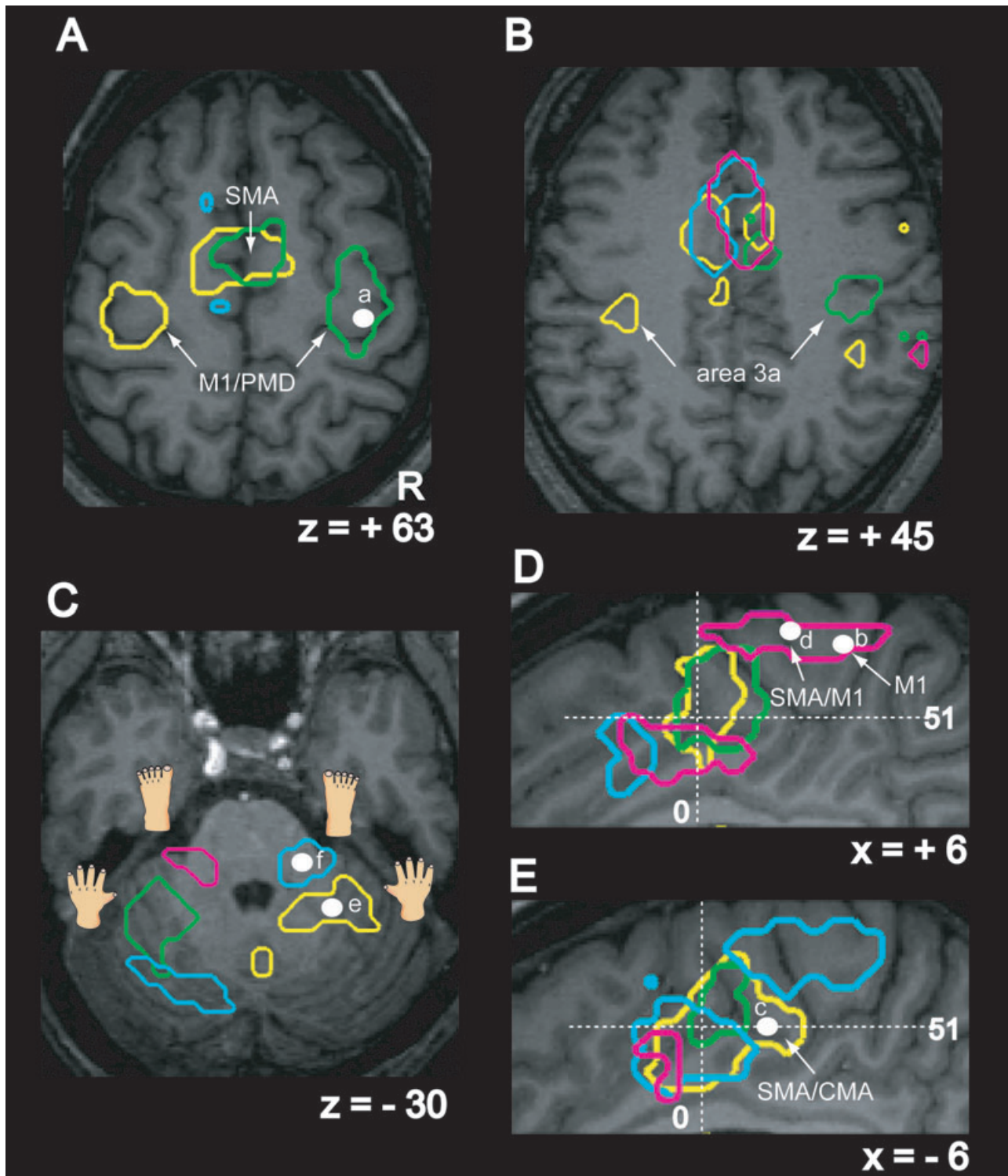


FIG. 1. Motor areas active during kinesthetic illusory movement of right hand (yellow), left hand (green), right foot (light blue), or left foot (pink). These areas were significantly activated during ILLUSION compared with VIBRATION for each limb. Right hemisphere is shown on the right. (A) Contralateral hand section of M1 and bilateral SMA were activated. Horizontal image ($z = +63$) is displayed. (B) Contralateral fundus of central sulcus (area 3a) was also activated during illusory hand movement. $z = +45$. (C) Ipsilateral hand or foot sections of cerebellum were activated. $z = -30$. In the section active in the left cerebellum during right foot illusion (light blue), we also found increased activity during illusions for the other three limbs (right hand, left hand, and left foot; $P > 0.001$ uncorrected), thus this section was not limb-specific. (D) Medial aspect of right hemisphere. $x = +6$. (E) Medial aspect of left hemisphere. $x = -6$. Vertical dashed lines indicate $y = 0$, and horizontal lines $z = +51$. Data from white dots with small letters (a–f) in panels are shown in Fig. 4.

vs. illusions for left hand and foot, i.e. [right hand (ILLUSION vs. VIBRATION) + right foot (ILLUSION vs. VIBRATION)] vs. [left hand (ILLUSION vs. VIBRATION) + left-foot (ILLUSION vs.

VIBRATION)]. In the second level analysis, the ROI was the regions (left-sided rostral CMA and thalamus, bilateral inferior frontal cortices and basal ganglia, and right inferior parietal cortex) that were

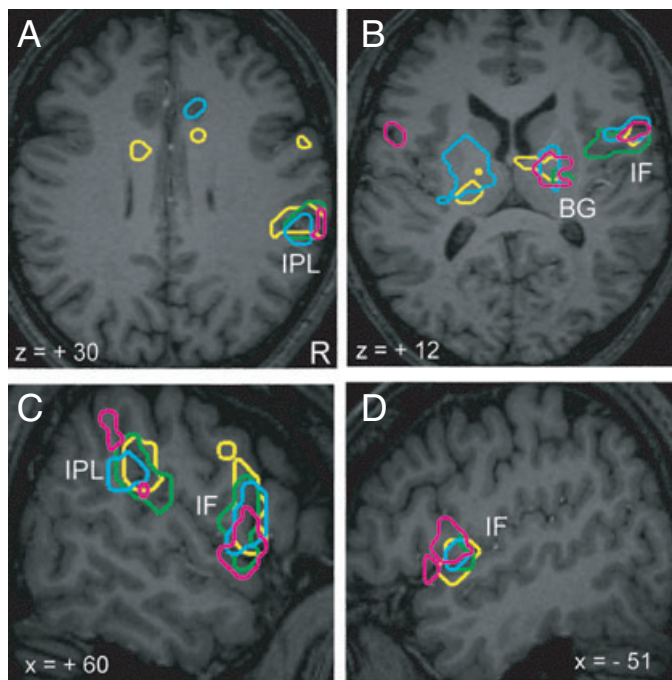


FIG. 2. Brain regions consistently active during illusion of each limb [right hand (yellow), left hand (green), right foot (blue), or left foot (pink)]. Right hemisphere is shown on the right. (A) Concentrated activations in right inferior parietal lobule (IPL) including cytoarchitectonic area ip1/dorsal part of parietal operculum (area op1; for anatomical definition see Table 1). Horizontal plane ($z = +30$) is displayed. (B) Activations in right inferior frontal (IF) cortex (area 44; see also Table 1) and basal ganglia (BG). $z = +12$. (C) Sagittal view of right inferior fronto-parietal activations is displayed ($x = +60$). (D) Sagittal view of left inferior frontal activation is displayed ($x = -51$).

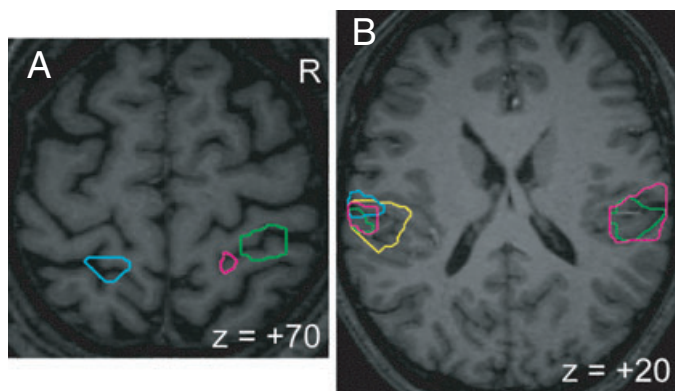


FIG. 3. Somatosensory areas active during skin vibration over a nearby bone of right hand (yellow), left hand (green), right foot (blue), or left foot (pink). These areas were significantly activated when VIBRATION was compared with REST for each limb. Right hemisphere is shown on the right. (A) $z = +70$. Contralateral postcentral sulcus regions were significantly active during skin vibration of left hand, right foot, and left foot. (B) $z = +20$. Skin vibration of all limbs also activated parietal operculum. None of areas shown in Figs 1 and 2 were significantly activated in either condition.

consistently active during right-hand illusion and during right-foot illusion.

The same procedure using a reversed contrast was performed to depict areas exclusively related to illusions for left-sided limbs (hand and foot). The ROI were the regions (right rostral CMA, inferior

frontal cortex, inferior parietal cortex, basal ganglia and thalamus) that were consistently active during illusions for left-sided limbs. These approaches ensure that activations detected exclusively reflect the illusions for limbs on the same (right or left) side of body as compared to the illusions for limbs on the other (left or right) side of body.

In addition, by applying a similar ROI approach as described above, we also examined regions exclusively active during illusions for a pair of right hand and left foot as compared to illusions for a pair of left hand and right foot, and also regions exclusively active during illusions for the latter pair of limbs by using a reversed contrast.

Finally, we investigated regions exclusively active during illusions for three particular limbs when compared with illusion for the rest of a limb, e.g. [right-hand (ILLUSION vs. VIBRATION) + left-hand (ILLUSION vs. VIBRATION)] + right-foot (ILLUSION vs. VIBRATION) vs. $3 \times$ left foot (ILLUSION vs. VIBRATION). The ROI were the regions that were consistently active during illusions for at least three limbs (bilateral rostral CMA and inferior frontal cortices, right inferior parietal, basal ganglia and thalamus; see Figs 1D and E, and 2). As none of these regions were exclusively activated during illusions for any trios of three particular limbs ($T < 3.61$), we examined whether all these regions were activated when we tested the main effect of illusions (see Table 1), i.e. right-hand (ILLUSION vs. VIBRATION) + left-hand (ILLUSION vs. VIBRATION) + right-foot (ILLUSION vs. VIBRATION) + left-foot (ILLUSION vs. VIBRATION).

To anatomically identify activation peaks, the locations were related to cytoarchitectonic 30% probability maps in the Montreal Neurological Institute reference brain space (www.bic.mni.mcgill.ca/cytoarchitectonics/; Mohlberg *et al.*, 2003; see also Naito *et al.*, 2002b, 2005; Naito & Ehrsson, 2006). For definitions of pre-SMA, SMA and CMA, we referred to Roland & Zilles (1996), and for the definition of cerebellar regions, we referred to the Schmahmann *et al.* (2000).

Percent increase in the BOLD signal in the ILLUSION condition as compared to the VIBRATION condition

We show per cent increase of the activity in the limb-specific (Table 2) and non-limb-specific regions (Fig. 5A) during illusions. First, we extracted the fMRI (8-mm filtered) data from local maxima in the

TABLE 1. Areas consistently active across illusions for all limbs

Brain areas	Coordinates of peaks			T-value	Cluster size (voxels)
	x	y	z		
Right inferior frontal cluster					
Anterior insula	45	3	3	11.4	289
Area 44	57	12	0	10.5	
Basal ganglia	27	6	-3	7.9	
Bilateral medial-wall cluster					
Left CMA rostral	-6	9	39	8.7	51
Right CMA rostral	6	6	48	5.7	
Right inferior parietal cluster					
Area op1	63	-30	30	7.7	46
Left inferior frontal cluster					
Area 44	-51	6	3	7.7	28

Voxel size, $3 \times 3 \times 3$ mm. Coordinates in Talairach & Tournoux (1988) as defined by MNI. Anatomical naming of the activated areas is based on coordinates of activation peaks (equals local maxima in a cluster > 8 mm apart). All these regions were consistently active during illusions for at least three limbs (Figs 1D and E, and 2) and were also activated ($T > 3.61$) as the main effect of illusions (see Materials and methods).

TABLE 2. Areas exclusively active during illusion for a particular limb in ROI analyses

Brain areas	Coordinates of peaks			T-value	Cluster size voxels
	x	y	z		
Right hand					
Left PMD-M1 cluster					
Area 6/4a	-33	-24	72	11.6	304
Area 4a	-33	-27	63	11.5	
Left medial-wall cluster					
SMA/CMA caudal	-6	-18	51	6.0	106
Area 6 (SMA)	-12	-12	57	5.5	
Right cerebellar cluster					
Lobe V	15	-60	-21	6.8	159
Lobe V	21	-51	-30	6.6	
Lobe V	18	-51	-21	6.5	
Left hand					
Right PMD-M1 cluster					
Area 4a/4p	33	-24	54	10.4	375
Area 4a	39	-27	60	9.8	
Area 6/4a	33	-24	72	9.6	
Right medial-wall cluster					
Area 6 (SMA) caudal	9	-15	54	4.7	6
Left cerebellar cluster					
Lobe VI	-27	-57	-33	6.6	61
Lobe V	-15	-54	-24	4.0	
Right foot					
Left SMA-M1 cluster					
Area 4a	-6	-36	78	9.3	157
Area 4a	-9	-39	69	8.8	
Area 4a/6	-6	-21	75	7.3	
Right cerebellar cluster					
Lobe III	15	-36	-33	6.4	67
Left foot					
Right SMA-M1 cluster					
Area 4a	6	-33	75	8.5	99
Area 4a/6	6	-21	78	6.7	
Left cerebellar cluster					
Lobe III	-18	-33	-27	7.6	46

T > 3.61, cluster size > 5 voxels. The atlas of the cerebellum is based on that of Schmahmann *et al.* (2000). See also note in Table 1.

limb-specific and non-limb-specific activations. This was performed separately for each participant. Then, we calculated a mean of BOLD signal for each epoch. The mean activity was calculated from six functional images in each epoch: we excluded the first two images (Naito *et al.*, 2005). This was carried out because the illusions started a few seconds after vibration onset and there must be a haemodynamic delay of several seconds. Next, we calculated percent increase in the BOLD signal in an ILLUSION epoch as compared to the corresponding VIBRATION epoch in a session using the following formula:

$$100 \times \frac{(\text{mean signal in an ILLUSION epoch} - \text{mean signal in the corresponding VIBRATION epoch})}{(\text{mean signal in the corresponding VIBRATION epoch})}$$

This was carried out for all three pairs of (ILLUSION and VIBRATION) epochs in a session. As two sessions including six pairs of epochs were assigned for each limb condition, we finally calculated a mean value of the per cent increase from the six values for each limb condition. We only report results from representative voxels in Figs 4 and 5.

To exclude the possibility that the results, particularly for the medial-wall activations (Fig. 5), merely reflect different degrees of

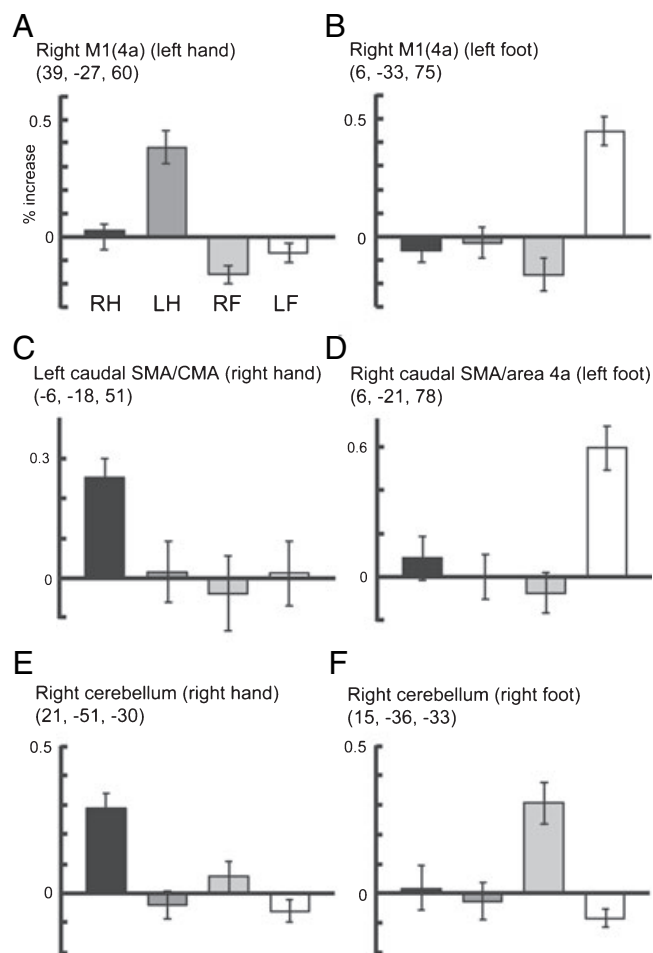


FIG. 4. Limb-specific activity in representative voxels of activations in contralateral M1 (A and B), SMA/CMA (C and D), and ipsilateral cerebellum (E and F), which were active during kinesthetic illusions (see also Fig. 1 and Table 2). Each panel A–F shows data from the corresponding voxels a–f in Fig. 1. RH, right hand; LH, left hand; RF, right foot; LF, left foot. These somatotopical regions were exclusively activated during a kinesthetic illusion of a particular limb. Bars indicate standard errors of means across participants.

spread of the activations due to the spatial filtering effect in the image processing (see above), we conducted the same analyses for the re-analysed fMRI data, which was smoothed using a 4-mm FWHM Gaussian filter. As the two results were identical, we only show the results from the latter analyses in Fig. 5.

Results

Behavioural experiments

No overt limb movements were observed during any trial in any vibration condition. Throughout the trials, all participants experienced vivid illusory movement when we vibrated the tendon (ILLUSION) and only the sensation of skin vibration when we vibrated the bone (VIBRATION) across all conditions. They reported that illusory wrist flexion movements (right hand, 23 ± 10 deg; left hand, 24 ± 11 deg) were larger than illusory ankle plantar-flexion movements (right foot, 6 ± 2 deg; left foot, 6 ± 3 deg). Two-factorial (right, left (2) × hand, foot (2); repeated measurement) ANOVA showed that illusory hand movement was significantly larger than illusory foot movement ($F_{1,18} = 47.8$, $P < 0.001$). Likewise, the onsets of illusory hand

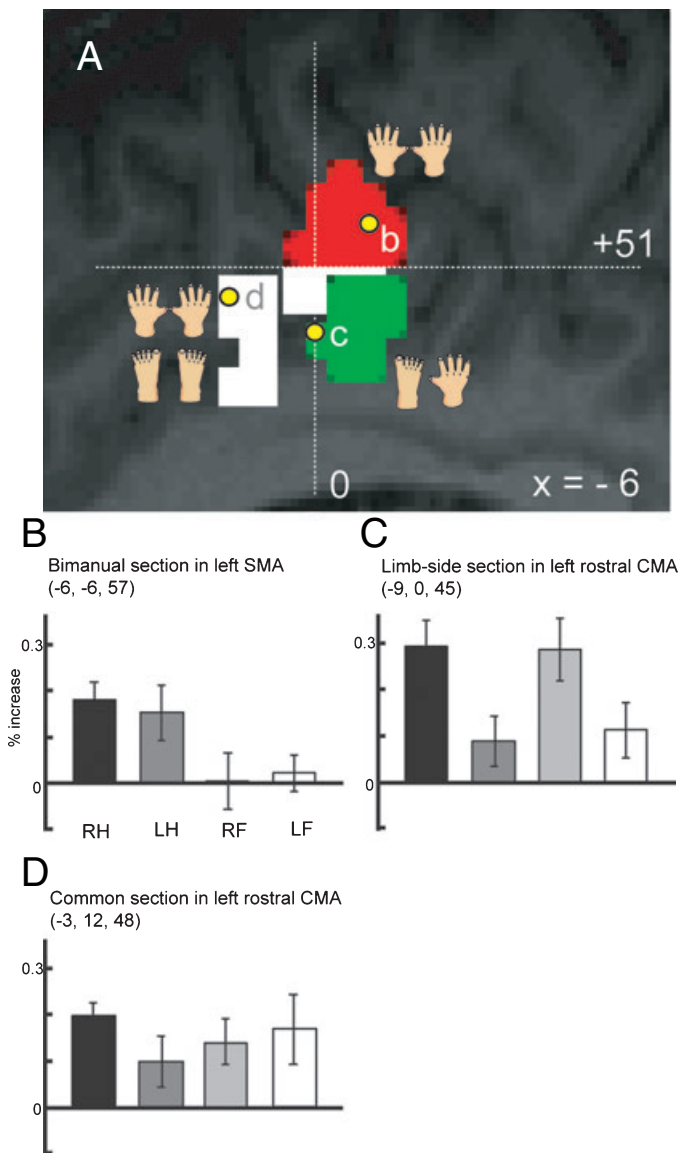


FIG. 5. Non-limb-specific regions in rostral parts of SMA and CMA. Sagittal view of left medial wall is displayed ($x = -6$). (A) Red section indicates bimanual section, green section for limb-side section, and white section for common section. Vertical dashed line indicate $y = 0$, and horizontal line $z = +51$. Per cent increase of activity during illusion is shown for each of three representative voxels (yellow dots with small letters b–d). (B) Activities in the bimanual section across illusions for all limbs. (C) Activities in the limb-side section during illusions for all limbs. (D) Activities in the common section. Bars indicate standard errors of means across participants.

movements (right hand, 2.2 ± 1.1 s; left hand, 2.0 ± 0.9 s) were significantly earlier than those of illusory foot movements (right foot, 3.7 ± 2.3 s; left foot, 3.8 ± 2.2 s; $F_{1,18} = 18.6$, $P < 0.001$). We also found a significant correlation for illusory angle between the right and left limbs across participants ($r = 0.81$, d.f. = 17, $P < 0.005$ between the hands; $r = 0.52$, $P < 0.05$ between the feet), meaning that a participant who felt a larger illusion for one hand or foot also felt a larger illusion for the other hand or foot. In contrast, no correlation was observed between hand and foot on the same side of body ($r = -0.02$ between right hand and foot; $r = 0.07$ between left hand and foot), suggesting that perception of upper limb movement is independent from that of lower limb movement.

In almost half (approximately 40%) of all trials, irrespective of the vibrated limb, there was absolutely no conspicuous muscular activity throughout the trial even when the participant consistently experienced vivid illusory limb movement. Even in the remaining trials, where we found an increase in either vibrated (ECU or TA) or agonistic (FCU or SO) muscle, the increase was temporal within the trial and rarely lasted throughout the tendon vibration. In the vibrated muscles, the increase was very small ($< 50 \mu\text{V}$) and lasted for a maximum of 10 s. In the agonistic (non-vibrated) muscles, the increase was even smaller ($< 20 \mu\text{V}$) and was often phasic (twitch-like). However, the angular magnitude of illusion did not significantly differ between trials with this occasional activity and those without [with EMG, 16 ± 13 deg; without EMG, 14 ± 11 deg (averages across illusions for all limbs); $P = 0.38$]. No activity was observed when the bone was vibrated.

fMRI experiment

After each fMRI session, all participants verbally reported that they experienced illusory flexion movement of the right or left hand when the ECU tendon of that hand was vibrated and illusory plantar-flexion of the right or left foot when the TA tendon of that foot was vibrated. After the experiment was completed, they retrospectively reported that they experienced larger illusions from the hand than from the foot during scanning, as they had in the behavioural experiment. No subjects reported any illusions for the VIBRATION sessions. The experimenter who was standing in the scanner room near the participant observed no overt movements of the participants' vibrated limbs in any condition. This observation was supported by the absence of conspicuous muscular activity in the behavioural experiment, and was consistent with our previous findings (Naito *et al.*, 1999, 2002a, b, 2005; Naito & Ehrsson, 2006).

Areas active during illusion (ILLUSION vs. VIBRATION)

Illusion for each limb activated cortical motor areas (M1, PMD, SMA and CMA), fronto-parietal cortices, cerebellum and basal ganglia (Figs 1 and 2). During hand illusions, the M1/PMD cluster extended into the fundus of the contralateral central sulcus (most probably somatosensory cytoarchitectonic area 3a; Fig. 1B).

The illusion for each limb consistently activated highly similar regions in bilateral rostral CMA (Fig. 1D and E; see also further below), bilateral inferior frontal cortices including area 44, right inferior parietal cortices including area ip1 and the dorsal part of the parietal operculum (PO, area op1), and right basal ganglia (Fig. 2). Indeed, all these regions were activated as the main effect of illusions (Table 1), and we confirmed in the ROI analyses that none of these regions were exclusively activated during illusions for any trios of three particular limbs ($T < 3.61$; see Materials and methods). Thus, the regions consistently active during illusions for at least three limbs can be considered as those consistently activated across illusions for all limbs (see Figs 2 and 5A white section). The right inferior frontal activation (Fig. 2C) was robust in size as compared to the left activation (Fig. 2D) as we found previously (Naito *et al.*, 2005; see cluster size in Table 1). The left basal ganglia was only activated during illusions for right-sided limbs, and its similar section was consistently activated during illusions for hand and foot (Fig. 2B).

Vibration of the skin over the nearby bone (beside the tendon) of each limb activated only the contralateral primary somatosensory cortex (areas 1, 2, and 3b) and parietal operculum (PO, area op1). None of the areas active during illusions were activated (Fig. 3).

Limb-specific activations related to illusions

Within the regions active during illusion of each limb (ILLUSION vs. VIBRATION; Fig. 1), regions exclusively active during illusion of a particular limb were identified in the somatotopical sections in the contralateral M1 (cytoarchitectonic areas 4a and 4p), PMD, caudal parts of SMA/CMA and in the ipsilateral cerebellum (Table 2). Figure 4 illustrates the per cent increase in the BOLD signal in the ILLUSION condition as compared to the VIBRATION condition in representative voxels of these regions. The activity in these motor areas increased exclusively during illusion for a particular limb, meaning that these activations were limb-specific.

Non-limb-specific activations in the medial wall during illusions

We found overlaps in activations in the rostral parts of the SMA and CMA across illusions (Fig. 1D and E). As described, the limb-specific sections were located in the caudal parts of the SMA and CMA (around $y < -9$; see Figs 1D and E, and 4C and D).

Anterior parts of the bilateral SMA (around $0 < y < -9$; $z > +51$) were exclusively activated during illusions for both right and left hands (red section in Fig. 5A). Activities in these regions specifically increased during illusions for right and left hands, but not during illusions for both feet (bimanual section; Fig. 5B). The bimanual section was only found in the SMA within the ROI (see Materials and methods). On the other hand, we only found 2 voxels in the midline parts of the bilateral SMA/M1 [peak coordinates ($x, y, z = 0, -21, 75$)] that were exclusively active during illusions for both right and left feet (bipedal section; not shown in figure).

We found that left rostral CMA (around $0 < y < -9$; $z < +51$) was exclusively activated during illusions for the right (contralateral) hand and foot as compared to the left (ipsilateral) hand and foot (green section in Fig. 5A). Likewise, the right corresponding section [peak coordinates ($x, y, z = 6, -9, 45$)] was also exclusively activated during illusions for left hand and foot (not shown in figure). Activities in these regions increased more during illusions for limbs on the contralateral side of body when compared with illusions for limbs on the ipsilateral side (limb-side section; Fig. 5C). Again, the limb-side section was only found in the medial wall within the ROI (see Materials and methods).

We found no regions (even in the entire ROI) exclusively active during illusions for right hand and left foot as compared to illusions for left hand and right foot *vice versa* ($T < 3.61$).

Finally, within the regions consistently active across illusions for all limbs (see Table 1 and also above), common activations in the medial wall were located in more anterior regions of bilateral CMA (around $y > 0$; $z < +51$; white section in Fig. 5A). The activities in these regions consistently increased (to the same extent) across illusions for all limbs (common section; Fig. 5D). The pre-SMA section (around > 0 ; $z > +51$) was relatively silent (Fig. 5A).

Discussion

Kinesthetic illusory movements of the upper and lower immobile extremities, i.e. right or left hand or foot, activated limb-specific sections of contralateral PMD/M1 (along with somatosensory area 3a) and caudal parts of the SMA/CMA, and ipsilateral cerebellum, which normally participate in execution of movements of the corresponding limb (cf. Penfield & Rasmussen, 1950). We found complex non-limb-specific representations in rostral parts of the bilateral SMA and CMA, and the illusion for each limb consistently engaged similar regions in right-sided fronto-parietal cortices and

basal ganglia. The kinesthetic function of multiple motor areas, which seems to be parallel to their executive function, suggests the importance of motor areas in the somatic perception of the dynamic configuration of our limbs (Fig. 1), and the non-limb-specific representations (Figs 1D and E, 2 and 5) indicate the hierarchical organization of human kinesthetic processing.

The limb-specific sections active during the illusion for each limb (Fig. 1 and Table 2) corresponded well to those active during execution of extension-flexion movement of the wrist or ankle [M1, right hand ($-40, -28, 64$), right foot ($-8, -28, 64$); caudal SMA, right foot ($-8, -20, 72$); caudal CMA, right hand ($-4, -24, 48$); cerebellum, right hand ($10, -50, -24$)] (Ehrsson *et al.*, 2000, 2003). Thus, it seems that kinesthetic processing of the muscle spindle afferent inputs (see Introduction) takes place in the multiple motor areas that normally participate in the generation of voluntary limb movement. This means that identical sections of multiple motor areas are engaged both in kinesthetic sensory processing and in the generation of corresponding limb movement (Weiller *et al.*, 1996; Thickbroom *et al.*, 2003; Ciccarelli *et al.*, 2005). As cells in these motor areas (M1/PM, Colebatch *et al.*, 1990; Porter & Lemon, 1993; SMA/CMA, Cadoret & Smith, 1995; cerebellum, van Kan *et al.*, 1993a, b) fire during active and passive movement of a limb in non-human primates, identical neurons in these motor areas may participate in both sensory processing and motor output. Thus, it is possible that the neuronal populations in these areas that generate motor activity also process kinesthetic signals related to the same movement. This functional organization could efficiently facilitate sensorimotor integration in human motor control.

Kinesthetic illusions for hand and foot movements

The amount of illusory hand movement was larger, and the time before its onset was shorter than that for illusory foot movement even when the tendons were vibrated with identical vibratory stimuli. It has been shown that the intensity of illusion is related to the number of muscle spindle afferent fibers that respond to a vibration frequency with a one-by-one recruitment pattern (Roll & Vedel, 1982; Roll *et al.*, 1989). Anatomically, the density of muscle spindles in human hand muscles is higher than that in leg muscles (Banks & Stacey, 1988). Thus, the psychophysical differences between hand and foot are most probably due to the difference in number of the afferents recruited by the vibratory stimuli.

We found a temporal increase of muscular activity in the vibrated (ECU or TA) or agonistic (FCU or SO) muscle during trials. In the present study, we used larger vibration amplitude (± 3.5 mm) to elicit vivid illusory foot movements than that previously used (± 2 mm) for the illusory hand movements (Naito *et al.*, 1999; Naito & Ehrsson, 2001; Naito *et al.*, 2002a, b, 2005). This may be why we observed a small increase in muscular activity in the behavioural experiment. However, neither the small temporal increase in the vibrated muscle that can be generated by spinal mechanisms mediating the tonic vibration reflex (TVR) (Eklund & Hagbarth, 1966; Marsden *et al.*, 1969; Naito *et al.*, 2002a), nor the twitch-like activity in the agonistic muscle, can be the main contributor to eliciting the illusory limb movement that was continuously experienced during tendon vibration. Further, the angular magnitude of illusion had nothing to do with the presence of occasional muscular activity. Thus, the muscular activity is not directly related to eliciting movement sensation during illusion. Together with our previous findings that the motor areas were consistently active when participants experienced vivid illusory hand movements with no significant increase of muscular activity (Naito

et al., 1999; Naito & Ehrsson, 2001; Naito *et al.*, 2002a, b, 2005), the present motor activations during illusions mainly participate in the kinesthetic processing of muscle spindle afferent inputs, but not merely in the generation of spontaneous motor activity.

Probably due to the tight coupling between kinesthetic processing and motor output in the motor areas (see above), the tendon vibration at the larger amplitude might have increased chances for cells in the motor areas to covertly contribute to the generation of subtle motor activity even though none of the participants intended to move. This paradoxically supports the claim we made above about the efficiency of the human motor system that facilitates motor output from the kinesthetic input.

The activations in the motor areas were only observed during illusions that are elicited by the central processing of the kinesthetic afferent inputs. Although the illusory hand movements activated the contralateral fundus of the central sulcus, i.e. somatosensory area 3a, as has been suggested in non-human primates (Hore *et al.*, 1976; Phillips *et al.*, 1971; Schwarz *et al.*, 1973; Iwamura *et al.*, 1983; Huerta & Pons, 1990; Huffman & Krubitzer, 2001), the somatosensory cortices (Fig. 3) were mainly activated by the passive skin vibration that may only excite vibro-tactile cutaneous receptors (vibrating the skin over the nearby bone beside the tendon only elicits the sensation of vibration but no reliable illusions). The somatosensory cortices are normally activated in the wide range of tasks that require cutaneous processing, e.g. shape, velocity, curvature, or roughness discrimination tasks (e.g. Bodegard *et al.*, 2000, 2001; Ledberg *et al.*, 1995; Roland *et al.*, 1998; Young *et al.*, 2004). Taken together, the present study seems to demonstrate the predominant involvement of motor areas in human kinesthesia (Fig. 1) that may contrast with the cutaneous function in the somatosensory cortices (Fig. 3), though human electrophysiological studies have suggested that motor and sensory functions can not be simply divided by the central sulcus (Penfield & Boldrey, 1937; Woolsey *et al.*, 1979; Nii *et al.*, 1996). The brain has to compute dynamic displacement of a limb during illusion, i.e. 'where is my limb moving', and when a cutaneous stimulus is applied, the brain has to analyse features of the stimulus to determine 'what is the stimulus'. Therefore, it seems that the 'where' function predominantly engages the motor network, which can be distinct from the cutaneous 'what' function in the somatosensory cortices (Naito, 2004a, b).

Functional organization of SMA and CMA during kinesthetic processing

We found limb-specific sections in the caudal parts of the SMA and CMA, and non-limb-specific sections of their rostral parts. The present spatial alignment of limb-specific sections of the SMA (see Fig. 1D and E) seems to correspond to SMA sites where electrical stimulation evokes the movements of lower or upper extremities in humans (Fried *et al.*, 1991; Lim *et al.*, 1994), in the sense that the lower extremities in the posterior region, whereas the upper extremities are represented in a relatively anterior region (Luft *et al.*, 2002). This finding seems to resemble a finding obtained in monkey studies (Mitz & Wise, 1987; He *et al.*, 1995); neurons in the caudal SMA connect to lower lumbosacral segments in the spinal cord, which control the lower extremities, whereas neurons in the relatively anterior SMA connect to the upper and lower cervical segments, which control the upper extremities (He *et al.*, 1995). Thus, together with our present kinesthetic representations in the human SMA, one may conjecture about the possibility of spatial correspondence between kinesthetic and motor representations in somatotopical sections of the human SMA (see above references).

We found regions that were active during illusions for both hands in the rostral part of the SMA (Fig. 5A and B). This is probably due to a dense interconnection between right and left SMA's, which is well known in non-human primates (Rouiller *et al.*, 1994; Tanji, 1994). We also found regions in the rostral part of the CMA that were active during illusions for both hand and foot on the same (contralateral) side of the body (Fig. 5A and C), and in a more anterior part of the CMA we found regions whose activities consistently increased across illusions for all limbs (Fig. 5A and D). It is unlikely that these complex representations merely reflect different degrees of the spread of activations in the medial wall due to the spatially smoothing effects of image processing because locally distinct peaks, which should have physiological importance (Picard & Strick, 1996), were identified in the activations, the data was obtained from the local maxima, and the results remained unchanged after the images were reprocessed using a smaller spatial filter (see Materials and methods), which reduces the spread of activation.

Lack of direct evidence about information flow within the SMA and CMA in the present fMRI study prevents us from drawing any conclusions, but it seems that limb-specific information in the caudal SMA and CMA (Fig. 1D and E) may converge to non-limb-specific sections of their rostral parts (Fig. 5A). As the rostral SMA has more dense transcallosal connections with frontal cortices than does the caudal SMA (Liu *et al.*, 2002), the concentration of the kinesthetic representations of all limbs in the rostral parts of the SMA and CMA may be efficient when the brain distributes kinesthetic information between the right and the left hemispheres (see further below).

A recent meta-analysis study has revealed that human frontal midline structures may have a function related to self-referencing of action and sensation (Seitz *et al.*, 2006). As a kinesthetic illusion elicited by tendon vibration requires people to be aware of change in their own limb position, it is also conceivable that part of the present medial-wall activations have something to do with high-order neuronal process related to kinesthetic self-referencing of changes of limb position. In addition, the non-limb-specific sections may play a supra-limb role in a situation that requires self-referencing of spatial relationship across limbs. Indeed, the non-limb-specific kinesthetic representations (sensory processing) seem to be useful when people perform sensory-motor tasks requiring interlimb coordination [e.g. hand-foot coordination (Ehrsson *et al.*, 2000) or bimanual coordination (Sadato *et al.*, 1997; Stephan *et al.*, 1999)]. The importance of the frontal midline structures in human interlimb coordination is supported by a finding that transcranial magnetic stimulation to the human SMA impairs bimanual coordination (Serrien *et al.*, 2002).

Activations in right fronto-parietal cortices and basal ganglia

The locations of concentrated activations in the right inferior frontal (area 44) and inferior parietal (areas ip1 and op1) cortices during illusions for all limbs (Fig. 2) corresponded to those in the right-dominant fronto-parietal activations during illusions for the right and left hands (see Naito *et al.*, 2005 for further discussions). Thus, these activations seem to be common across illusions for all limbs.

Although motor imagery of various types of hand movements also often activates the right inferior frontal cortex (area 44), activity in the right inferior parietal cortex is not always associated with the imagery (Binkofski *et al.*, 2000; Gerardin *et al.*, 2000; Ehrsson *et al.*, 2003; Lotze & Halsband, 2006). Thus, right frontal-parietal coactivation seems to be a typical activation pattern during illusory limb movements elicited by the sensory processing of peripheral kinesthetic inputs. In addition, the right-sided activations during illusions fit well

with human brain lesion studies, demonstrating that damage to the right inferior frontal and parietal cortices impairs perception of one's own body (Berlucchi & Aglioti, 1997; Hyvärinen, 1982; Sellal *et al.*, 1996; Damasio, 1999; Berti *et al.*, 2005; Committeri *et al.*, 2007).

We cannot completely deny the possibility that the present right-sided activations are related to a general function, e.g. spatial attention to limb movements, due to lack of a perfect control condition that is attentionally comparable to ILLUSION condition in the present study (ILLUSION can be more attention-grabbing condition as compared to VIBRATION with no illusion). But, together with the heterogeneous patterns in activations between motor imagery (also requires spatial attention to limb movements) and kinesthetic illusion and with the neurological evidences described above, the present right-sided activations consistently observed across illusions for all limbs may reflect, at least partly, high-order sensory processing probably related to neuronal computation of supra-limb kinesthetic representation, for example, updating of the neuronal representation of human somatic perception of one's own body (Committeri *et al.*, 2007).

The present robust activations in the basal ganglia (BG) are novel in our series of studies. In the present study, we scanned brain activity in 19 participants, which may increase sensitivity to detect the brain signals when compared with our previous studies where we scanned the activity in a maximum of 12 participants. Human BG is an important constituent of the motor network that controls our limb movements (e.g. Lehericy *et al.*, 2006) and dysfunction of the BG (Parkinson's disease) impairs kinesthesia/proprioception (Lidsky *et al.*, 1985; Schneider *et al.*, 1987; Klockgether *et al.*, 1995; Zia *et al.*, 2000, 2002; Maschke *et al.*, 2003). Thus, the BG seems to participate in the kinesthetic processing and awareness of limb position. In monkeys, it has been shown that the BG has complex somatotopical organization by forming predominantly ipsilateral loops with the somatotopical sections of the cortical motor (M1, PM, SMA and CMA) areas (Middleton & Strick, 2000; Nambu *et al.*, 1996, 1997; Takada *et al.*, 1998, 2001) and BG cells exhibit short-latency (sensory) neuronal responses to passive joint rotation, and it is suggested that this sensory information is probably transmitted through the cerebral cortices (Delong *et al.*, 1985). Hence, the present BG activations, particularly contralateral to the vibrated limbs (typically the left BG activations during illusions for right hand and foot; see Fig. 2B), could be driven by the inputs from the cortical motor areas (Fig. 1), even though the limitations of spatial resolution in the present fMRI study prevented us from depicting clear somatotopical organization in the BG (Fig. 2B).

We found more complex and concentrated activations in the right BG across illusions for all limbs. The activations during illusions for left limbs may be partly explained by the cortical inputs described above. In monkeys, the BG forms a predominantly ipsilateral loop with the rostral ventral premotor cortex (PMV; Nambu *et al.* 1997; Takada *et al.*, 1998), which has been suggested to be a homologue region of human area 44 (e.g. Rizzolatti *et al.*, 2002; Binkofski & Buccino, 2006), and the monkey's PMV is connected to the inferior parietal cortices (Ghosh & Gattera, 1995; Godschalk *et al.*, 1984; Neal *et al.*, 1990), which are also connected to the BG (Clower *et al.*, 2005). Thus, the present right BG activations may have some relation to the right fronto-parietal activations (cf. Middleton & Strick, 2000). Neuronal activity in human area 44 represents both hand (Buccino *et al.*, 2001; Binkofski & Buccino, 2006; as in a monkey's PMV; see Dum & Strick, 2005; He *et al.*, 1993) and foot (Ehrsson *et al.*, 2000, 2003). Thus, if the present right-sided activations form a brain network, the network could be involved in high-order bodily functions irrespective of the limb. The claim that the human BG is a constituent of the network related to high-order bodily functions may be partly

supported by a neurological finding that patients with hemi-Parkinson's disease are impaired in relating their internal representation of perceived body size to an aperture width external to their body, indicating that the human BG may have a function that closely mimics the parietal one (Lee *et al.*, 2001).

In conclusion, the illusory movements of the four extremities engage limb-specific sections of multiple motor areas (Fig. 1A–C and Table 2) and non-limb-specific regions in the rostral parts of the SMA/CMA (Figs 1D and E, and 5) and in the right fronto-parietal cortices and basal ganglia (Fig. 2). The present study demonstrated complete sets of brain representations related to kinesthetic processing of single-joint movements of the four human extremities.

Acknowledgements

The authors are grateful to Dr Shintaro Funahashi for his comments on the earlier version of this manuscript. This research was partially supported by the Ministry of Education, Science, Sports and Culture, Grant-in-Aid for Scientific Research (C), 17500209, 2005, and partly by the 21st Century COE Program (D-2 to Kyoto University) of MEXT Japan, and partly by the Brain Science Foundation.

Abbreviations

BG, basal ganglia; BOLD, blood oxygenation-level dependent; CMA, cingulate motor area; ECU, extensor carpi ulnaris; FCU, flexor carpi ulnaris; fMRI, functional magnetic resonance imaging; M1, primary motor cortex; PMD, dorsal premotor cortex; PO, parietal operculum; ROI, regions-of-interest; SMA, supplementary motor area; SO, soleus; TA, tibialis anterior.

References

- Banks, R. & Stacey, M. (1988) Quantitative studies on mammalian muscle spindles and their sensory innervation. In Hnik, P., Soukup, T., Vejsada, R. & Zelena, J., (Eds), *Mechanoreceptors: Development, Structure, and Function*. Plenum, New York, pp. 263–269.
- Bard, C., Fleury, M., Teasdale, N., Paillard, J. & Nougier, V. (1995) Contribution of proprioception for calibrating and updating the motor space. *Can. J. Physiol. Pharmacol.*, **73**, 246–254.
- Berlucchi, G. & Aglioti, S. (1997) The body in the brain: neural bases of corporeal awareness. *TINS*, **20**, 560–564.
- Berti, A., Bottini, G., Gandola, M., Pia, L., Smania, N., Stracciari, A., Castiglioni, I., Vallar, G. & Paulesu, E. (2005) Shared cortical anatomy for motor awareness and motor control. *Science*, **309**, 488–491.
- Binkofski, F., Amunts, K., Stephan, K.M., Posse, S., Schormann, T., Freund, H.J., Zilles, K. & Seitz, R.J. (2000) Broca's region subserves imagery of motion: a combined cytoarchitectonic and fMRI study. *Hum. Brain Mapp.*, **11**, 273–285.
- Binkofski, F. & Buccino, G. (2006) The role of ventral premotor cortex in action execution and action understanding. *J. Physiol. (Paris)*, **99**, 396–405.
- Bodegard, A., Geyer, S., Grefkes, C., Zilles, K. & Roland, P.E. (2001) Hierarchical processing of tactile shape in the human brain. *Neuron*, **31**, 317–328.
- Bodegard, A., Geyer, S., Naito, E., Zilles, K. & Roland, P.E. (2000) Somatosensory areas in man activated by moving stimuli: cytoarchitectonic mapping and PET. *Neuroreport*, **11**, 187–191.
- Buccino, G., Binkofski, F., Fink, G.R., Fadiga, L., Fogassi, L., Gallese, V., Seitz, R.J., Zilles, K., Rizzolatti, G. & Freund, H.J. (2001) Action observation activates premotor and parietal areas in a somatotopic manner: an fMRI study. *Eur. J. Neurosci.*, **13**, 400–404.
- Burgess, P.R., Wei, J.Y., Clark, F.J. & Simon, J. (1982) Signalling of kinesthetic information by peripheral sensory receptors. *Ann. Rev. Neurosci.*, **5**, 171–187.
- Burke, D., Gandevia, S.C. & Macefield, G. (1988) Responses to passive movement of receptors in joint, skin and muscle of the human hand. *J. Physiol.*, **402**, 347–361.
- Burke, D., Hagbarth, K., Lofstedt, L. & Wallin, G. (1976) The responses of human muscle spindle endings to vibration of non-contracting muscles. *J. Physiol. (Lond.)*, **261**, 673–693.

- Cadoret, G. & Smith, A.M. (1995) Input-output properties of hand-related cells in the ventral cingulate cortex in the monkey. *J. Neurophysiol.*, **73**, 2584–2590.
- Ciccarelli, O., Toosy, A.T., Marsden, J.F., Wheeler-Kingshott, C.M., Sahyoun, C., Matthews, P.M., Miller, D.H. & Thompson, A.J. (2005) Identifying brain regions for integrative sensorimotor processing with ankle movements. *Exp. Brain Res.*, **166**, 31–42.
- Clower, D.M., Dum, R.P. & Strick, P.L. (2005) Basal ganglia and cerebellar inputs to 'AIP'. *Cereb. Cortex*, **15**, 913–920.
- Colebatch, J.G., Sayer, R.J., Porter, R. & White, O.B. (1990) Responses of monkey precentral neurones to passive movements and phasic muscle stretch: relevance to man. *Electroencephalogr. Clin. Neurophysiol.*, **75**, 44–55.
- Collins, D.F., Refshauge, K.M., Todd, G. & Gandevia, S.C. (2005) Cutaneous receptors contribute to kinesthesia at the index finger, elbow, and knee. *J. Neurophysiol.*, **94**, 1699–1706.
- Committeri, G., Pitzalis, S., Galati, G., Patria, F., Pelle, G., Sabatini, U., Castriota-Scanderbeg, A., Piccardi, L., Guariglia, C. & Pizzamiglio, L. (2007) Neural bases of personal and extrapersonal neglect in humans. *Brain*, **130**, 431–441.
- Damasio, A.R. (1999) *The Feeling of What Happens: Body and Emotion in the Making of Consciousness*. Harcourt Brace, New York.
- Delong, M.R., Crutcher, M.D. & Georgopoulos, A.P. (1985) Primate globus pallidus and subthalamic nucleus: Functional organization. *J. Neurophysiol.*, **53**, 530–543.
- Dum, R.P. & Strick, P.L. (2005) Frontal lobe inputs to the digit representations of the motor areas on the lateral surface of the hemisphere. *J. Neurosci.*, **25**, 1375–1386.
- Edin, B.B. (2004) Quantitative analyses of dynamic strain sensitivity in human skin mechanoreceptors. *J. Neurophysiol.*, **92**, 3233–3243.
- Edin, B.B. & Abbs, J.H. (1991) Finger movement responses of cutaneous mechanoreceptors in the dorsal skin of human hand. *J. Neurophysiol.*, **65**, 657–670.
- Edin, B.B. & Johansson, N. (1995) Skin strain patterns provide kinaesthetic information to the human central nervous system. *J. Physiol.*, **487**, 243–251.
- Edin, B.B. & Vallbo, Å.B. (1988) Stretch sensitization of human muscle spindles. *J. Physiol.*, **400**, 101–111.
- Edin, B.B. & Vallbo, Å.B. (1990) Dynamic response of human muscle spindle afferents to stretch. *J. Neurophysiol.*, **63**, 1297–1306.
- Ehrsson, H.H., Geyer, S. & Naito, E. (2003) Imagery of voluntary movement of fingers, toes, and tongue activates corresponding body-part-specific motor representations. *J. Neurophysiol.*, **90**, 3304–3316.
- Ehrsson, H.H., Naito, E., Geyer, S., Amunts, K., Zilles, K., Forssberg, H. & Roland, P.E. (2000) Simultaneous movements of upper and lower limbs are coordinated by motor representations that are shared by both limbs: a PET study. *Eur. J. Neurosci.*, **12**, 3385–3398.
- Eklund, G. & Hagbarth, K.E. (1966) Normal variability of tonic vibration reflexes in man. *Exp. Neurol.*, **16**, 80–92.
- Fried, I., Katz, A., McCarthy, G., Sass, K.J., Williamson, P., Spencer, S.S. & Spencer, D.D. (1991) Functional organization of human supplementary motor cortex studied by electrical stimulation. *J. Neurosci.*, **11**, 3656–3666.
- Friston, K.J., Holmes, A.P. & Worsley, K.J. (1999) How many subjects constitute a study? *Neuroimage*, **10**, 1–5.
- Gandevia, S.C. (1985) Illusory movements produced by electrical stimulation of low-threshold muscle afferents from the hand. *Brain*, **108**, 965–981.
- Gerardin, E., Sirigu, A., Lehericy, S., Poline, J.B., Gaymard, B., Marsault, C., Agid, Y. & Bihan, D.L. (2000) Partially overlapping neural networks for real and imagined hand movements. *Cereb. Cortex*, **10**, 1093–1104.
- Ghez, C. & Sainburg, R. (1995) Proprioceptive control of interjoint coordination. *Can. J. Physiol. Pharmacol.*, **73**, 273–284.
- Ghosh, S. & Gattera, R.A. (1995) Comparison of the ipsilateral cortical projections to the dorsal and ventral subdivisions of the macaque premotor cortex. *Somatosens. Mot. Res.*, **12**, 359–378.
- Godschalk, M., Lemon, R.N., Kuypers, H.G.J.M. & Ronday, H.K. (1984) Cortical afferents and efferents of monkey postarcuate area: an anatomical and electrophysiological study. *Exp. Brain Res.*, **56**, 410–424.
- Goodwin, G.M., McCloskey, D.I. & Matthews, P.B.C. (1972a) The contribution of muscle afferents to kinesthesia shown by vibration induced illusions of movement and by the effects of paralysing joint afferents. *Brain*, **95**, 705–748.
- Goodwin, G.M., McCloskey, D.I. & Matthews, P.B.C. (1972b) Proprioceptive illusions induced by muscle vibration: Contribution by muscle spindles to perception? *Science*, **175**, 1382–1384.
- He, S.Q., Dum, R.P. & Strick, P.L. (1993) Topographic organization of corticospinal projections from the frontal lobe: Motor areas on the lateral surface of the hemisphere. *J. Neurosci.*, **13**, 952–980.
- He, S.Q., Dum, R.P. & Strick, P.L. (1995) Topographic organization of corticospinal projections from the frontal lobe: motor areas on the medial surface of the hemisphere. *J. Neurosci.*, **15**, 3284–3306.
- Head, H. & Holmes, G. (1911) Sensory disturbances from cerebral lesions. *Brain*, **34**, 102–254.
- Hore, J., Preston, J.B., Durkovic, R.G. & Cheney, P.D. (1976) Responses of cortical neurons (areas 3a and 4) to ramp stretch of hindlimb muscles in the baboon. *J. Neurophysiol.*, **39**, 484–500.
- Huerta, M.F. & Pons, T.P. (1990) Primary motor cortex receives input from area 3a in macaque. *Brain Res.*, **537**, 367–371.
- Huffman, K.J. & Krubitzer, L. (2001) Area 3a: topographic organization and cortical connections in marmoset monkeys. *Cereb. Cortex*, **11**, 849–867.
- Hyvärinen, J. (1982) *Studies of Brain Function. The Parietal Cortex of Monkey and Man*. Springer-Verlag, Berlin.
- Iwamura, Y., Tanaka, M., Sakamoto, M. & Hikosaka, O. (1983) Functional subdivisions representing different finger regions in area 3 of the first somatosensory cortex of the conscious monkey. *Exp. Brain Res.*, **51**, 315–326.
- Johansson, R.S. & Vallbo, A.B. (1983) Tactile sensory coding in the glabrous skin of the human hand. *TINS*, **6**, 27–32.
- van Kan, P.L.E., Gibson, A.R. & Houk, J.C. (1993b) Movement-related inputs to intermediate cerebellum of the monkey. *J. Neurophysiol.*, **69**, 74–94.
- van Kan, P.L.E., Houk, J.C. & Gibson, A.R. (1993a) Output organization of intermediate cerebellum of the monkey. *J. Neurophysiol.*, **69**, 57–73.
- Kito, T., Hashimoto, T., Yoneda, T., Katamoto, S. & Naito, E. (2006) Sensory processing during kinesthetic aftereffect following hand movement elicited by tendon vibration. *Brain Res.*, **1114**, 75–84.
- Klockgether, T., Borutta, M., Rapp, H., Spieker, S. & Dichgans, J. (1995) A defect of kinesthesia in Parkinson's disease. *Mov. Disord.*, **10**, 460–465.
- Ledberg, A., O'Sullivan, B.T., Kinomura, S. & Roland, P.E. (1995) Somatosensory activations of the parietal operculum of man. A PET study. *Eur. J. Neurosci.*, **7**, 1934–1941.
- Lee, A.C., Harris, J.P., Atkinson, E.A. & Fowler, M.S. (2001) Disruption of estimation of body-scaled aperture width in Hemiparkinson's disease. *Neuropsychologia*, **39**, 1097–1104.
- Lehericy, S., Bardin, E., Tremblay, L., Van de Moortele, P.F., Pochon, J.B., . . . Dormont, D., Kim, D.S., Yelnik, J. & Ugurbil, K. (2006) Motor control in basal ganglia circuits using fMRI and brain atlas approaches. *Cereb. Cortex*, **16**, 149–161.
- Lidsky, T.L., Manetto, C. & Schneider, J.S. (1985) A consideration of sensory factors involved in motor functions of the basal ganglia. *Brain Res.*, **356**, 133–146.
- Lim, S.H., Dinner, D.S., Pillay, P.K., Luders, H., Morris, H.H., Klem, G., Wyllie, E. & Awad, I.A. (1994) Functional anatomy of the human supplementary sensorimotor area: results of extraoperative electrical stimulation. *Electroencephalogr. Clin. Neurophysiol.*, **91**, 179–193.
- Liu, J., Morel, A., Wannier, T. & Rouiller, E.M. (2002) Origins of callosal projections to the supplementary motor area (SMA): a direct comparison between pre-SMA and SMA-proper in macaque monkeys. *J. Comp. Neurol.*, **443**, 71–85.
- Lotze, M. & Halsband, U. (2006) Motor imagery. *J. Physiol. (Paris)*, **99**, 386–395.
- Luft, A.R., Smith, G.V., Forrester, L., Whittall, J., Macko, R.F., Hauser, T.K., Goldberg, A.P. & Hanley, D.F. (2002) Comparing brain activation associated with isolated upper and lower limb movement across corresponding joints. *Hum. Brain Mapp.*, **17**, 131–140.
- Marsden, C.D., Meadows, J.C. & Hodgson, H.J.F. (1969) Observations on the reflex response to muscle vibration in man and its voluntary control. *Brain*, **92**, 829–846.
- Maschke, M., Gomez, C.M., Tuite, P.J. & Konczak, J. (2003) Dysfunction of the basal ganglia, but not the cerebellum, impairs kinaesthesia. *Brain*, **126**, 2312–2322.
- Matthews, P.B.C. (1982) Where does Sherrington's 'Muscular sense' originate? Muscles, joints, corollary discharges? *Ann. Rev. Neurosci.*, **5**, 189–218.
- Middleton, F.A. & Strick, P.L. (2000) Basal ganglia and cerebellar loops: motor and cognitive circuits. *Brain Res. Rev.*, **31**, 236–250.
- Mitz, A.R. & Wise, S.P. (1987) The somatotopic organization of the supplementary motor area: intracortical microstimulation mapping. *J. Neurosci.*, **7**, 1010–1021.
- Mohlberg, H., Lerch, J., Amunts, K., Evans, A. & Zilles, K. (2003) Probabilistic cytoarchitectonic maps transformed into MNI space. *Hum. Brain Mapp.*, **19**, Abstract 905, New York, June 21, Academic Press, St. Louis.

- Naito, E. (2004a) Sensing limb movements in the motor cortex: How humans sense limb movement. *Neuroscientist*, **10**, 73–82.
- Naito, E. (2004b) Imaging human somatosensory systems. *Shinkei Kenkyu No Shinpo*, **48**, 249–260.
- Naito, E. & Ehrsson, H.H. (2001) Kinesthetic illusion of wrist movement activates motor-related areas. *Neuroreport*, **12**, 3805–3809.
- Naito, E. & Ehrsson, H.H. (2006) Somatic sensation of hand-object interactive movement is associated with activity in the left inferior parietal cortex. *J. Neurosci.*, **26**, 3783–3790.
- Naito, E., Ehrsson, H.H., Geyer, S., Zilles, K. & Roland, P.E. (1999) Illusory arm movements activate cortical motor areas: a positron emission tomography study. *J. Neurosci.*, **19**, 6134–6144.
- Naito, E., Kochiyama, T., Kitada, R., Nakamura, S., Matsumura, M., Yonekura, Y. & Sadato, N. (2002a) Internally simulated movement sensations during motor imagery activate the cortical motor areas and the cerebellum. *J. Neurosci.*, **22**, 3683–3691.
- Naito, E., Roland, P.E. & Ehrsson, H.H. (2002b) I feel my hand moving: a new role of the primary motor cortex in somatic perception of limb movement. *Neuron*, **36**, 979–988.
- Naito, E., Roland, P.E., Grefkes, C., Choi, H.J., Eickhoff, S., Geyer, S., Zilles, K. & Ehrsson, H.H. (2005) Dominance of the right hemisphere and role of area 2 in human kinesthesia. *J. Neurophysiol.*, **93**, 1020–1034.
- Nambu, A., Takada, M., Inase, M. & Tokuno, H. (1996) Dual somatotopical representations in the primate subthalamic nucleus: Evidence for ordered but reversed body-map transformations from the primary motor cortex and the supplementary motor area. *J. Neurosci.*, **16**, 2671–2683.
- Nambu, A., Tokuno, H., Inase, M. & Takada, M. (1997) Corticostriatal input zones for forelimb representations of the dorsal and ventral divisions of the premotor cortex in the macaque monkey: comparison with the input zones from the primary motor cortex and the supplementary motor area. *Neurosci. Lett.*, **239**, 13–16.
- Neal, J.W., Pearson, R.C. & Powell, T.P. (1990) The ipsilateral corticocortical connections of area 7 with the frontal lobe in the monkey. *Brain Res.*, **509**, 31–40.
- Nii, Y., Uematsu, S., Lesser, R.P. & Gordon, B. (1996) Does the central sulcus divide motor and sensory functions: Cortical mapping of human hand areas as revealed by electrical stimulation through subdural grid electrodes. *Neurology*, **46**, 360–367.
- Oldfield, R.C. (1971) The assessment and analysis of handedness: the Edinburgh inventory. *Neuropsychologia*, **9**, 97–113.
- Penfield, W. & Boldrey, E. (1937) Somatic motor and sensory representation in the cerebral cortex of man as studied by electrical stimulation. *Brain*, **60**, 389–443.
- Penfield, W. & Rasmussen, T. (1950) *The Cerebral Cortex of Man: a Clinical Study of Localization of Function*. Macmillan, New York.
- Phillips, C.G., Powell, T.P.S. & Wiesendanger, M. (1971) Projection from low threshold muscle afferents of hand and forearm to area 3a of baboon's cortex. *J. Physiol. (Lond.)*, **217**, 419–446.
- Picard, N. & Strick, P.L. (1996) Motor areas of the medial wall: a review of their location and functional activation. *Cereb. Cortex*, **6**, 342–353.
- Porter, R. & Lemon, R.N. (1993) Inputs from the peripheral receptors to motor cortex neurones. In *Corticospinal Function and Voluntary Movement*. Oxford University Press, New York, pp. 247–272.
- Ribot-Ciscar, E. & Roll, J.P. (1998) Ago-antagonist muscle spindle inputs contribute together to joint movement coding in man. *Brain Res.*, **791**, 167–176.
- Rizzolatti, G., Fogassi, L. & Gallese, V. (2002) Motor and cognitive functions of the ventral premotor cortex. *Curr. Opin. Neurobiol.*, **12**, 149–154.
- Roland, P.E., O'Sullivan, B. & Kawashima, R. (1998) Shape and roughness activate different somatosensory areas in the human brain. *Proc. Natl Acad. Sci. USA*, **95**, 3295–3300.
- Roland, P.E. & Zilles, K. (1996) Functions and structures of the motor cortices in humans. *Curr. Opin. Neurobiol.*, **6**, 773–781.
- Roll, J.P. & Vedel, J.P. (1982) Kinaesthetic role of muscle afferent in man, studied by tendon vibration and microneurography. *Exp. Brain Res.*, **47**, 177–190.
- Roll, J.P., Vedel, J.P. & Ribot, E. (1989) Alteration of proprioceptive messages induced by tendon vibration in man: a microneurographic study. *Exp. Brain Res.*, **76**, 213–222.
- Rothwell, J.C., Traub, M.M., Day, B.L., Obeso, J.A., Thomas, P.K. & Marsden, C.D. (1982) Manual motor performance in a deafferented man. *Brain*, **105**, 515–542.
- Rouiller, E.M., Babalian, A., Kazennikov, O., Moret, V., Yu, X.H. & Wiesendanger, M. (1994) Transcallosal connections of the distal forelimb representations of the primary and supplementary motor cortical areas in macaque monkeys. *Exp. Brain Res.*, **102**, 227–243.
- Sadato, N., Yonekura, Y., Waki, A., Yamada, H. & Ishii, Y. (1997) Role of the supplementary motor area and the right premotor cortex in the coordination of bimanual finger movements. *J. Neurosci.*, **17**, 9667–9674.
- Sainburg, R.L., Ghilardi, M.F., Poizner, H. & Ghez, C. (1995) Control of limb dynamics in normal subjects and patients without proprioception. *J. Neurophysiol.*, **73**, 820–835.
- Schmahmann, J.D., Doyon, J., Toga, A.W., Petrides, M. & Evans, A.C. (2000) *MRI Atlas of the Human Cerebellum*. Academic press, San Diego.
- Schneider, J.S., Diamond, S.G. & Markham, C.H. (1987) Parkinson's disease: sensory and motor problems in arms and hands. *Neurology*, **37**, 951–956.
- Schwarz, D.W.F., Deecke, L. & Fredrickson, J.M. (1973) Cortical projection of group I muscle afferents to area 2, 3a and the vestibular field in the rhesus monkey. *Exp. Brain Res.*, **17**, 516–526.
- Seitz, R.J., Nickel, J. & Azari, N.P. (2006) Functional modularity of the medial prefrontal cortex: involvement in human empathy. *Neuropsychology*, **20**, 743–751.
- Sellal, F., Renaseau-Leclerc, C. & Labrecque, R. (1996) The man with six arms. An analysis of supernumerary phantom limbs after right hemisphere stroke. *Rev. Neurol. (Paris)*, **152**, 190–195.
- Serrien, D.J., Strens, L.H., Oliviero, A. & Brown, P. (2002) Repetitive transcranial magnetic stimulation of the supplementary motor area (SMA) degrades bimanual movement control in humans. *Neurosci. Lett.*, **328**, 89–92.
- Stephan, K.M., Binkofski, F., Halsband, U., Dohle, C., Wunderlich, G., Schnitzler, A., Tass, P., Posse, S., Herzog, H., Sturm, V., Zilles, K., Seitz, R.J. & Freund, H.J. (1999) The role of ventral medial wall motor areas in bimanual co-ordination. A combined lesion and activation study. *Brain*, **122**, 351–368.
- Takada, M., Tokuno, H., Hamada, I., Inase, M., Ito, Y., Imanishi, M., Hasegawa, N., Akazawa, T., Hatanaka, N. & Nambu, A. (2001) Organization of inputs from cingulate motor areas to basal ganglia in macaque monkey. *Eur. J. Neurosci.*, **14**, 1633–1650.
- Takada, M., Tokuno, H., Nambu, A. & Inase, M. (1998) Corticostriatal projections from the somatic motor areas of the frontal cortex in the macaque monkey: segregation versus overlap of input zones from the primary motor cortex, the supplementary motor area, and the premotor cortex. *Exp. Brain Res.*, **120**, 114–128.
- Talairach, J. & Tournoux, P. (1988) *A Co-Planar Stereotaxic Atlas of a Human Brain*. Thieme, New York.
- Tanji, J. (1994) The supplementary motor area in the cerebral cortex. *Neurosci. Res.*, **19**, 251–268.
- Thickbroom, G.W., Byrnes, M.L. & Mastaglia, F.L. (2003) Dual representation of the hand in the cerebellum: activation with voluntary and passive finger movement. *Neuroimage*, **18**, 670–674.
- Weiller, C., Juptner, M., Fellows, S., Rijntjes, M., Leonhardt, G., Kiebel, S., Müller, S., Diener, H.C. & Thilmann, A.F. (1996) Brain representation of active and passive movements. *Neuroimage*, **4**, 105–110.
- Wiesendanger, M. & Miles, T.S. (1982) Ascending pathway of low-threshold muscle afferents to the cerebral cortex and its possible role in motor control. *Physiol. Rev.*, **62**, 1234–1270.
- Woolsey, C.N., Erickson, T.C. & Gilson, W.E. (1979) Localization in somatic sensory and motor areas of human cerebral cortex as determined by direct recording of evoked potentials and electrical stimulation. *J. Neurosurg.*, **51**, 476–506.
- Young, J.P., Herath, P., Eickhoff, S., Choi, H.J., Grefkes, C., Zilles, K. & Roland, P.E. (2004) Somatotopy and attentional modulation of the human parietal and opercular regions. *J. Neurosci.*, **24**, 5391–5399.
- Zia, S., Cody, F.W. & O'Boyle, D. (2000) Joint position sense is impaired by Parkinson's disease. *Ann. Neurol.*, **47**, 218–228.
- Zia, S., Cody, F.W. & O'Boyle, D.J. (2002) Identification of unilateral elbow joint position is impaired by Parkinson's disease. *Clin. Anat.*, **15**, 23–31.